AMERICAN SOCIETY FOR MICROBIOLOGY | Infection and Immunity

Fur Represses Adhesion to, Invasion of, and Intracellular Bacterial Community Formation within Bladder Epithelial Cells and Motility in Uropathogenic *Escherichia coli*

Kumiko Kurabayashi,[a] Tomohiro Agata,[a] Hirofumi Asano,[a] Haruyoshi Tomita,[b,c] Hidetada Hirakawa[a]

Advanced Scientific Research Leaders Development Unit,[a] Department of Bacteriology,[b] and Laboratory of Bacterial Drug Resistance,[c] Gunma University, Graduate School of Medicine, Showa-machi, Maebashi, Gunma, Japan

Uropathogenic *Escherichia coli* (UPEC) is a major pathogen that causes urinary tract infections (UTIs). This bacterium adheres to and invades the host cells in the bladder, where it forms biofilm-like polymicrobial structures termed intracellular bacterial communities (IBCs) that protect UPEC from antimicrobial agents and the host immune systems. Using genetic screening, we found that deletion of the *fur* gene, which encodes an iron-binding transcriptional repressor for iron uptake systems, elevated the expression of type I fimbriae and motility when UPEC was grown under iron-rich conditions, and it led to an increased number of UPEC cells adhering to and internalized in bladder epithelial cells. Consequently, the IBC colonies that the *fur* mutant formed in host cells were denser and larger than those formed by the wild-type parent strain. Fur is inactivated under iron-restricted conditions. When iron was depleted from the bacterial cultures, wild-type UPEC adhesion, invasion, and motility increased, similar to the case with the *fur* mutant. The purified Fur protein bound to regions upstream of *fimA* and *flhD*, which encode type I fimbriae and an activator of flagellar expression that contributes to motility, respectively. These results suggest that Fur is a repressor of *fimA* and *flhD* and that its repression is abolished under iron-depleted conditions. Based on our *in vitro* experiments, we conclude that UPEC adhesion, invasion, IBC formation, and motility are suppressed by Fur under iron-rich conditions but derepressed under iron-restricted conditions, such as in patients with UTIs.

Uropathogenic *Escherichia coli* (UPEC) is an extraintestinal *E. coli* organism which infects the urinary tract. Urinary tract infection (UTI) is one of the most common diseases, and it is estimated that over 80% of uncomplicated UTIs are caused by UPEC (1, 2). In the initial stage of infection, UPEC migrates to the bladder, where it adheres to and may invade epithelial cells, in which it forms biofilm-like polymicrobial colonies termed intracellular bacterial communities (IBCs) (3, 4). After the bacteria ascend the ureters and reach the kidneys, if untreated or if chemotherapy fails, this may result in septicemia. Therefore, adherence to the bladder epithelial cells is a key step to determine whether infection becomes refractory to treatment, because the entry of UPEC into the bladder epithelial cells is followed by IBC formation that is able to escape from the host immune systems. These bacteria may exhibit tolerance to antimicrobials (5, 6).

Previous studies suggested that fimbriae and motility are important to establish the infections for UPEC. The type 1 fimbria encoded by *fim* genes is a major fimbria for this bacterium. It is required for the initial attachment, invasion, and IBC formation in the bladder epithelial cells (7, 8). In addition, motility contributes bacterial migration to the infection sites and also fitness when the bladder is colonized (9–11).

Iron is a cofactor for many primary and secondary metabolic enzymes, but it may also generate reactive hydroxyl radicals, which, at high levels, can cause oxidative damage to cells (12). Therefore, the intracellular iron concentration is strictly controlled by an iron-binding global regulator, Fur (ferric uptake regulator) (13, 14). The Fur protein forms a complex with ferrous iron and represses the expression of a subset of genes encoding iron uptake systems such as siderophore biosynthetic enzymes and receptors, and it then blocks incorporation of excess iron. However, once available, iron is restricted, the Fur protein is shifted to an iron-free inactive state, and then the target genes are derepressed.

In this study, we aimed to identify genes that are responsible for adherence, invasion, and/or IBC formation in bladder epithelial cells to help understand the regulation of UPEC virulence and identify new drug targets for treating this infectious disease. We performed a random transposon mutagenesis and found that the *fur* gene may be involved in the control of adhesion, invasion, and IBC formation. The *fur* mutant demonstrated increased adhesion, resulting in higher invasion and IBC formation in the bladder epithelial cells, and was associated with higher expression levels of *fim* genes, which encode the type 1 fimbriae, than was the wild-type parent when grown in an iron-rich medium. Deletion of the *fur* gene also increased expression of the *fliC* gene, which encodes a flagellar component, and led to elevated motility. Fur bound to the regions upstream of *fimA* and *flhD* genes, which encode a major subunit of type 1 fimbriae and an activator of *fliC* expression, respectively. Fur-mediated suppression of these phenotypes

Received 29 April 2016 **Returned for modification** 1 June 2016
Accepted 24 August 2016

Accepted manuscript posted online 29 August 2016

Citation Kurabayashi K, Agata T, Asano H, Tomita H, Hirakawa H. 2016. Fur represses adhesion to, invasion of, and intracellular bacterial community formation within bladder epithelial cells and motility in uropathogenic *Escherichia coli*. Infect Immun 84:3220–3231. doi:10.1128/IAI.00369-16.

Editor: S. M. Payne, University of Texas at Austin

Address correspondence to Hidetada Hirakawa, hirakawa@gunma-u.ac.jp.

Supplemental material for this article may be found at http://dx.doi.org/10.1128/IAI.00369-16.

TABLE 1 Strains and plasmids used in this study

Strain or plasmid	Relevant genotype or phenotype[a]	Reference
Strains		
CFT073	Wild-type parent strain (ATCC 700928)	15
CFT073 Δ*fur*	*fur* mutant of CFT073	This work
CFT073 Δ*ryhB*	*ryhB* mutant of CFT073	This work
CFT073 Δ*lrp*	*lrp* mutant of CFT073	This work
CFT073 Δ*fur* Δ*lrp*	*fur lrp* mutant of CFT073	This work
CFT073 Δ*fur* Δ*ryhB*	*fur ryhB* mutant of CFT073	This work
Plasmids		
pKO3	Temperature-sensitive vector for gene targeting; *sacB*; Cm^r	17
pTrc99A	Vector for IPTG-inducible expression; Ap^r	18
pTrc99Afur	Fur overexpression plasmid; Ap^r	This work
pTrc99Afur6His	C-terminal Fur-His_6 overexpression plasmid; Ap^r	This work
pTrc99AryhB	RyhB overexpression plasmid; Ap^r	This work
pUC19	Very-high-copy-number plasmid; Ap^r	19
pUC19ryhB	RyhB overexpression plasmid; Ap^r	This work
pTurboGFP-B	GFP expression plasmid; Ap^r	Evrogen

[a] Cm^r, chloramphenicol resistance; Ap^r, ampicillin resistance.

was alleviated when Fur was inactivated by growth in iron-depleted medium. Thus, these results suggest that adhesion, invasion, IBC formation, and motility of UPEC are suppressed by Fur under iron-rich conditions, but they are derepressed under iron-restricted conditions, such as infection of bladder cells.

MATERIALS AND METHODS

Bacterial strains, host cells, and culture conditions. Bacterial strains and plasmids used in this study are listed in Table 1. UPEC strain CFT073 (15) and derivatives were cultured in Luria-Bertani (LB) or RPMI 1640 (Sigma-Aldrich, St. Louis, MO) medium without shaking. Cell growth was monitored as the optical density at 600 nm (OD_{600}). For marker selection and maintaining plasmids, antibiotics were added to growth media at following concentrations: ampicillin, 150 μg/ml; chloramphenicol, 45 μg/ml; and kanamycin, 50 μg/ml. To heterologously express *fur* and *ryhB* from an isopropyl-β-D-thiogalactopyranoside (IPTG)-inducible promoter on plasmids, we added 0.01 mM IPTG to the culture media. HTB-9 bladder epithelial cells (16) were cultured in RPMI 1640 medium containing 10% HyClone FetalClone III serum (HyClone Laboratories, Inc., Logan, UT) at 37°C under 5% CO_2.

Random mutagenesis. To perform random mutagenesis, we used the EZ-Tn5 <RKrori/KAN-2>TNP Transposome kit (Epicentre, Madison, WI). The transposon was introduced into UPEC strain CFT073 as described by the manufacturer.

Cloning and mutant constructions. In-frame deletion of *fur* was constructed by sequence overlap extension PCR using a strategy described previously (17), with primer pairs delta1/delta2 and delta3/delta4 as listed in Table 2. The upstream flanking DNA included 450 bp and the first three amino acid codons. The downstream flanking DNA included the last three amino acid codons, the stop codon, and 450 bp of DNA. The deletion construct was ligated into BamHI- and SalI-digested temperature-sensitive vector pKO3 (17) and introduced into CFT073, the wild-type parent strain. We selected sucrose-resistant, chloramphenicol-sensitive colonies at 30°C and confirmed the resulting mutant strains using PCR analysis and DNA sequencing. We also constructed each mutant with a deletion of the *ryhB* or *lrp* gene by the same method using primer pairs ryhB-delta1/ryhB-delta2 and ryhB-delta3/ryhB-delta4 or lrp-delta1/lrp-delta-2 and lrp-delta3/lrp-delta4. The *ryhB* gene was deleted except for the first 13 nucleotides, while the *lrp* gene was deleted except for first and last three amino acid codons from start and stop codons, respectively.

To construct IPTG-inducible Fur, C-terminally histidine-tagged Fur, and RyhB expression plasmids pTrc99Afur, pTrc99Afur6His, and pTrc99AryhB, respectively, we PCR amplified the *fur* and *ryhB* genes with the primer pair shown in Table 2. These products were digested with NcoI and SalI for the *fur* gene and EcoRI and HindIII for the *ryhB* gene and ligated into similarly digested pTrc99A plasmids (18). We also cloned the *ryhB* gene into high-copy-number plasmid pUC19 (19). The *ryhB* gene was amplified with ryhB-F and ryhB-R primers. The product was digested with BamHI and HindIII and ligated into similarly digested pUC19 plasmid. All constructs were confirmed by DNA sequencing.

Static biofilm assays. The capability for bacterial adhesion and biofilm formation was quantified by a static biofilm assay using crystal violet as described elsewhere, with slight modifications (20). Bacteria were cultured for 24 h at 37°C in LB medium without shaking. Each culture was diluted into LB or RPMI 1640 medium at a 1:100 ratio, and ~2.4×10^4 cells were seeded into a 96-well polystyrene plate in triplicate. The plate was incubated at 37°C under 5% CO_2. Attached and biofilm cells on the plate were stained with crystal violet, and the A_{595} for each well was measured. The capability for attachment and biofilm formation was determined as the A_{595} normalized to an OD_{600} of 1.

Biofilm imaging on confocal microscopy. Bacteria were cultured on glass coverslips in 6-well polystyrene plates at 37°C under 5% CO_2 in RPMI 1640 medium. The coverslips were washed five times with phosphate-buffered saline (PBS) and stained with 5 μM Syto9 (Life Technologies, Carlsbad, CA) for 10 min. The coverslips were washed twice and fixed with 4% paraformaldehyde in PBS before mounting on glass slides with Fluoromount/Plus (Diagnostic BioSystems, Pleasanton, CA). Fluorescent images were acquired in the Alexa Fluor 488 laser unit on an Olympus FV1200 IX81 microscope using a 60× objective and captured with a charge-coupled-device (CCD) camera.

Infection of bladder epithelial cells. Bacterial adherence to and invasion of bladder epithelial cells were evaluated by gentamicin protection assays as described previously (7). HTB-9 cells were cultured to confluence in 24-well plates and were inoculated with a multiplicity of infection (MOI) of 10 bacteria per host cell in triplicate wells. After incubation at 37°C for 2 h, the cells in a first set of triplicate wells were lysed by 0.1% Triton X-100 for determining the total number of bacteria. The number of adhered/invaded bacteria was determined by counting the bacteria present in a second set of wells after washing five times with PBS+ (PBS containing 0.5 mM Mg^{2+} and 1 mM Ca^{2+}). To determine the number of invaded bacteria only, we washed a third set of wells twice with PBS+ after initial incubation and incubated them in the presence of gentamicin at 100 μg/ml for another 2 h at 37°C. The wells were washed three times with

TABLE 2 Primers used in this study

Primer	DNA sequence (5′–3′)	Use
fur-delta1	GCGGGATCCCGGGCTACCACTTCGAAGC	*fur* mutant construction
fur-delta2	TCAGGCTGGCTTATTTGCCTTCGTTATCAGTCATGCGGAATC	*fur* mutant construction
fur-delta3	CAGATTCCGCATGACTGATAACGAAGGCAAATAAGCCAGCC	*fur* mutant construction
fur-delta4	GCGGTCGACGCGGCAGGTTTTGTGCCTG	*fur* mutant construction
ryhB-delta1	GGGAGTCGACACAGATACC	*ryhB* mutant construction
ryhB-delta2	TTACACCTTAGCGCAAAGCGGACGGGTCTTCCTGATCGCGAG	*ryhB* mutant construction
ryhB-delta3	TTGTCTCGCGATCAGGAAGACCCGTCCGCTTTGCGCTAAGGTG	*ryhB* mutant construction
ryhB-delta4	GCGGGATCCACGGCGTAACGATCAGCCC	*ryhB* mutant construction
lrp-delta1	GCGGGATCCCAATCGGCAGCATCGATAAGC	*lrp* mutant construction
lrp-delta2	CTGTTCCGTGTTAGCGCGTCTTGCTATCTACCATTATTATTGTC	*lrp* mutant construction
lrp-delta3	GACAATAATAATGGTAGATAGCAAGACGCGCTAACACGGAAC	*lrp* mutant construction
lrp-delta4	GCGGTCGACATTCGTCGCTGGACTGATGAC	*lrp* mutant construction
pTrc-fur-F	GCGCCATGGCTGATAACAATACCGCC	pTrc99Afur construction
pTrc-fur-R	GCGGTCGACTTATTTGCCTTCGTGCGCG	pTrc99Afur construction
pTrc-fur-6His-R	GCGGTCGACTTAGTGATGGTGATGGTGATGTTTGCCTTCGTGCGCGTGC	pTrc99Afur6His construction
pTrc-ryhB-F	GCGGAATTCGTGTTGGACAAGTGCGAATG	pTrc99AryhB construction
pTrc-ryhB-R	GCGAAGCTTAAAGCGGACGTGGTTCCTAC	pTrc99AryhB construction
ryhB-F	GCGAAGCTTTGTTTCTGCGTGGCGTATTAC	pUC19ryhB construction
ryhB-R	GCGGGATCCAAAGCGGACGTGGTTCCTAC	pUC19ryhB construction
rrsA-qPCR-F	CGGTGGAGCATGTGGTTTAA	Quantitative real-time PCR
rrsA-qPCR-R	GAAAACTTCCGTGGATGTCAAGA	Quantitative real-time PCR
rpoD-qPCR-F	CAAGCCGTGGTCGGAAAA	Quantitative real-time PCR
rpoD-qPCR-R	GGGCGCGATGCACTTCT	Quantitative real-time PCR
fimA-qPCR-F	TGCGGGTAGCGCAACAA	Quantitative real-time PCR
fimA-qPCR-R	ACGCAGTCCCTGTTTTATCCA	Quantitative real-time PCR
fimH-qPCR-F	GATGCGGGCAACTCGATT	Quantitative real-time PCR
fimH-qPCR-R	CCCTGCGCGGGTGAA	Quantitative real-time PCR
papA-qPCR-F	TTTTTCGGGTGTCCCAAGTG	Quantitative real-time PCR
papA-qPCR-R	TGTTGCACCGACGGTCTGT	Quantitative real-time PCR
papG-qPCR-F	GGGAGGGAATGTGGTGATTACTC	Quantitative real-time PCR
papG-qPCR-R	CGGGCGCCACGAAGT	Quantitative real-time PCR
flhD-qPCR-F	GACAACGTTAGCGGCACTGA	Quantitative real-time PCR
flhD-qPCR-R	TTGATTGGTTTCTGCCAGCTT	Quantitative real-time PCR
fliA-qPCR-F	CGAGCGTGGAACTTGACGAT	Quantitative real-time PCR
fliA-qPCR-R	CGACGGCATTAAGTAACCCAAT	Quantitative real-time PCR
fliC-qPCR-F	TCCACTGAAAGCTCTGGATGAA	Quantitative real-time PCR
fliC-qPCR-R	CCCAGGGATGAACGGAATT	Quantitative real-time PCR
fim-phase-F	GAGAAGAAGCTTGATTTAACTAATTG	Phase variation assay
fim-phase-F	AGAGCCGCTGTAGAACTCAGG	Phase variation assay

PBS+, and the cells were lysed by 0.1% Triton X-100 and plated for CFU determination.

We also imaged the intracellular bacterial community (IBC) of UPEC formed in HTB-9 cells on a confocal microscope. The UPEC strain CFT073 carrying a green fluorescent protein (GFP) expression plasmid, pTurboGFP-B (Evrogen, Moscow, Russia), was inoculated with an MOI of 10 bacteria per host cell into cultured HTB-9 cells on glass coverslips in a 6-well plate and incubated at 37°C for 2 h. As for gentamicin protection assays, noninvading bacteria were washed out with gentamicin and PBS+. The HTB-9 cells on glass coverslips were stained with 0.16 μM Rhodamine phalloidin (Life Technologies, Carlsbad, CA) for 20 min. The coverslips were washed twice and fixed with 4% paraformaldehyde in PBS before mounting on glass slides with Fluoromount/Plus. Fluorescent images were acquired in the Alexa Fluor 488 for GFP-expressing bacteria and rhodamine phalloidin for HTB-9 cells laser units on an Olympus FV1200 IX81 microscope using a 60× objective and captured with a CCD camera.

RNA extraction and quantitative real-time PCR analyses. Bacteria were cultured for 24 h at 37°C in LB medium without shaking. Each culture was diluted into RPMI 1640 medium at a 1:100 ratio and incubated for 4 h (to late logarithmic growth phase; $OD_{600} \sim 0.5$). Total RNA extraction and cDNA synthesis were performed using an SV total RNA isolation system and GoScript reverse transcription system as described by the manufacturer (Promega Corp., Madison, WI). Real-time PCR included 2.5 ng of cDNA and 200 nM primers in SYBR Select master mix (Applied Biosystems, Foster City, CA) and was run on an ABI Prism 7900HT fast real-time PCR system. Constitutively expressed *rrsA* and *rpoD* genes were used as internal controls. Primers are listed in Table 2. Amplification plot and melting curve data are available upon request.

HA assays. To assess the activity of type 1 pili, we tested the hemagglutination (HA) of guinea pig red blood cells (RBCs) in PBS. Bacteria were statically cultured at 37°C under 5% CO_2 in RPMI 1640 medium and harvested in duplicate tubes. The cell pellets in a first tube were resuspended in PBS, while those in the other tube were resuspended in PBS containing 1% mannose and incubated for 10 min at room temperature. These resuspensions were serially diluted in 96-well round-bottom plates containing PBS, and an equal volume of 1% RBC suspension was added. After incubation for 4 h at 4°C, HA titers were determined. The titers were represented as the reciprocal of the last dilution well before RBC buttons were formed.

Phase variation assays. PCR-based phase variation assays for *fim* gene were performed as described by Struve and Krogfelt, with slight modifications (21). Bacteria were statically cultured at 37°C under 5% CO_2 in

RPMI 1640 medium. Cells were harvested and resuspended in PBS to an OD_{600} of 1. After boiling and centrifugation, the lysed supernatant was used as a template for PCR. For the assays, we PCR amplified the region upstream of *fim* gene operon with fim-phase-F and fim-phase-R primers, and 80 ng of PCR fragment was digested with HinfI. The DNA samples were separated by electrophoresis on a 5% nondenaturing acrylamide Tris-glycine-EDTA (10 mM Tris [pH 8.0], 380 mM glycine, and 1 mM EDTA) gel in Tris-glycine-EDTA buffer. The gel was then incubated with 10,000-fold-diluted SYBR green I nucleic acid stain (Lonza, Walkersville, MD), and the DNA was visualized under UV light at 300 nm.

Motility assays. RPMI 1640 medium containing 0.3% agar was spotted with 2 μl of bacteria grown for 24 h at 37°C in LB medium. Bacterial motility was evaluated by measuring the motility diameters after 8 h at 37°C under 5% CO_2.

Overexpression and purification of Fur. C-terminally histidine-tagged Fur (Fur-His_6) was expressed in and purified from *Escherichia coli* Rosetta(DE3) (Novagen/EMD Bioscience, Philadelphia, PA). Bacteria containing recombinant plasmid were cultured at 37°C to an OD_{600} of 0.4 in LB medium, 0.5 mM IPTG was then added, and culture growth was continued for 3 h. Cells were harvested and stored at −80°C overnight. To lyse the cells, the cell pellet was suspended in BactYeastLysis buffer including proteinase inhibitor, DNase, and lysozyme (ATTO, Tokyo, Japan) and incubated for 10 min. An equal volume of purification buffer (25 mM Tris [pH 7.5], 100 mM NaCl, 2 mM dithiothreitol, and 10% glycerol) was added to the lysate, and the mixture was centrifuged. The resulting supernatant was mixed with nickel-nitrilotriacetic acid (Ni-NTA) agarose (Qiagen, Valencia, CA) for 1 h. The agarose was washed twice with 10 mM imidazole and once with 50 mM imidazole, and Fur-His_6 was then eluted with 200 mM imidazole. Purified protein was desalted with Zeba desalt spin columns (Thermo Scientific, Rockford, IL) and eluted with buffer for the gel shift assays (20 mM Tris [pH 7.5], 50 mM KCl, 1 mM dithiothreitol, 100 μM $MnCl_2$, and 10% glycerol). The protein was >95% pure as estimated by SDS-PAGE electrophoresis and Coomassie brilliant blue staining. The protein concentration was determined using a Bio-Rad protein assay (Bio-Rad, Hercules, CA).

Gel shift assays. To assess Fur binding to *fimA*, *flhD*, *fliA*, and *fliC* promoter sequences in gel shift assays, we used a 462-bp DNA probe containing the 441-bp region upstream of the *fimA* start codon and 321-bp DNA probes containing the 300-bp regions upstream of the *flhD*, *fliA*, and *fliC* start codons, respectively. We also used a 323-bp DNA fragment from the *torC* gene as a nonspecific control probe. The DNA probes (0.30 pmol) were mixed with purified Fur-His_6 in a 10-μl reaction mixture. After incubation for 20 min at room temperature, samples were separated by electrophoresis on a 5% nondenaturing acrylamide Tris-glycine-$MnCl_2$ (10 mM Tris [pH 8.0], 380 mM glycine, and 100 μM $MnCl_2$) gel in Tris-glycine-$MnCl_2$ buffer at 4°C. The gel was incubated with 10,000-fold-diluted SYBR green I nucleic acid stain (Lonza, Walkersville, MD), and the DNA was visualized under UV light at 300 nm.

Statistical analyses. Statistical analyses were performed using unpaired *t* tests and two-way analysis of variance (ANOVA) with GraphPad Prism version 6.00. A *P* value of <0.05 was considered significant.

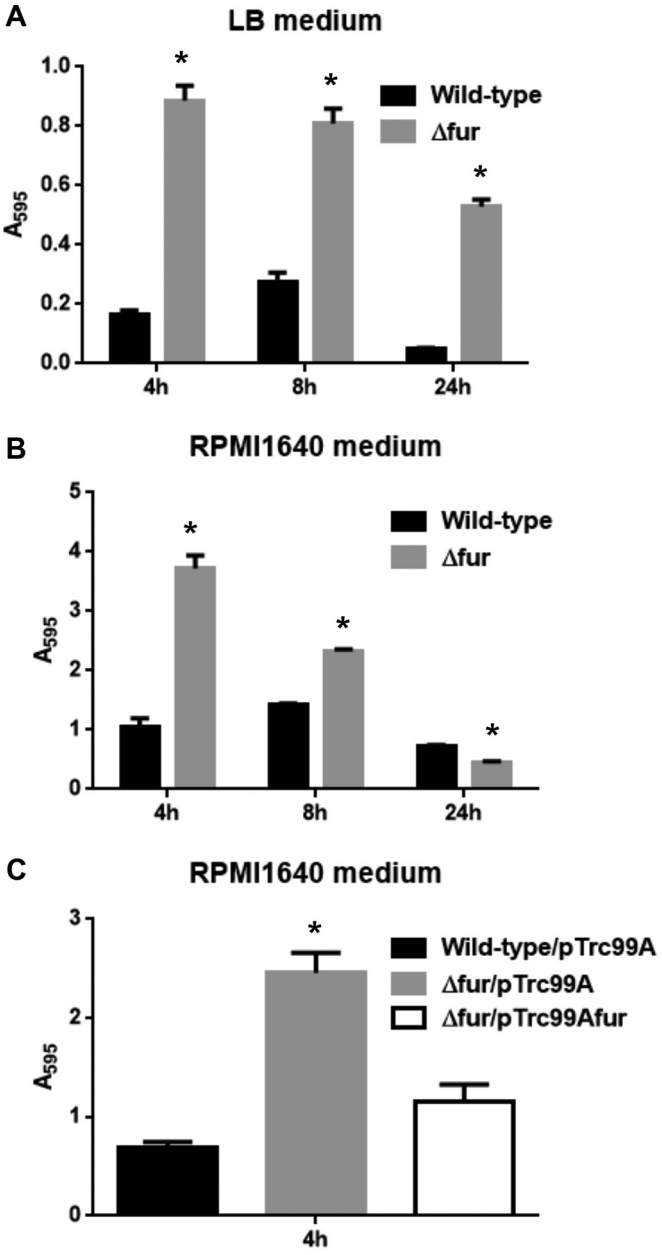

FIG 1 Rates of attached bacteria on 96-well polystyrene plates in the wild-type parent and the *fur* mutant when cultured in LB medium (A) or RPMI 1640 medium (B) or in the wild-type parent and the *fur* mutant carrying pTrc99A (vector control) or pTrc99Afur (Fur expression plasmid) when cultured in RPMI 1640 medium (C). These rates are represented as A_{595} values normalized to an OD_{600} of 1. Data are the means of three biological replicates; error bars indicate the ranges. *, $P < 0.01$ relative to the value for the wild-type control.

RESULTS

Deletion of the *fur* gene increases attachment to polystyrene and glass surfaces. Initially, we searched for genes that contribute to UPEC adhesion, invasion, and/or IBC formation by performing static biofilm assays in 96-well polystyrene plates. The assays are often used to evaluate the capability for adhesion and biofilm formation (20). Based on our transposon-mediated random mutagenesis screen, we selected 2,000 colonies and performed static biofilm assays for bacteria cultured from each colony. We found that a clone with a transposon inserted into the *fur* gene exhibited a higher degree of attachment to the 96-well polystyrene plate than the wild-type parent when statically cultured in LB medium. To verify this result, we constructed an in-frame deletion mutant of the *fur* gene (Δ*fur*) as described in Materials and Methods. Similar to the original mutant isolated by transposon mutagenesis, the Δ*fur* strain was more adhesive than the wild-type parent (Fig. 1A). We repeated the assay in the tissue culture medium RPMI 1640, which is typically used for growing bladder epithelial cells. After culture for up to 8 h, the Δ*fur* strain exhibited increased attachment compared to that of the wild-type parent, but the number of attached mutant cells was less than half that for the wild-type

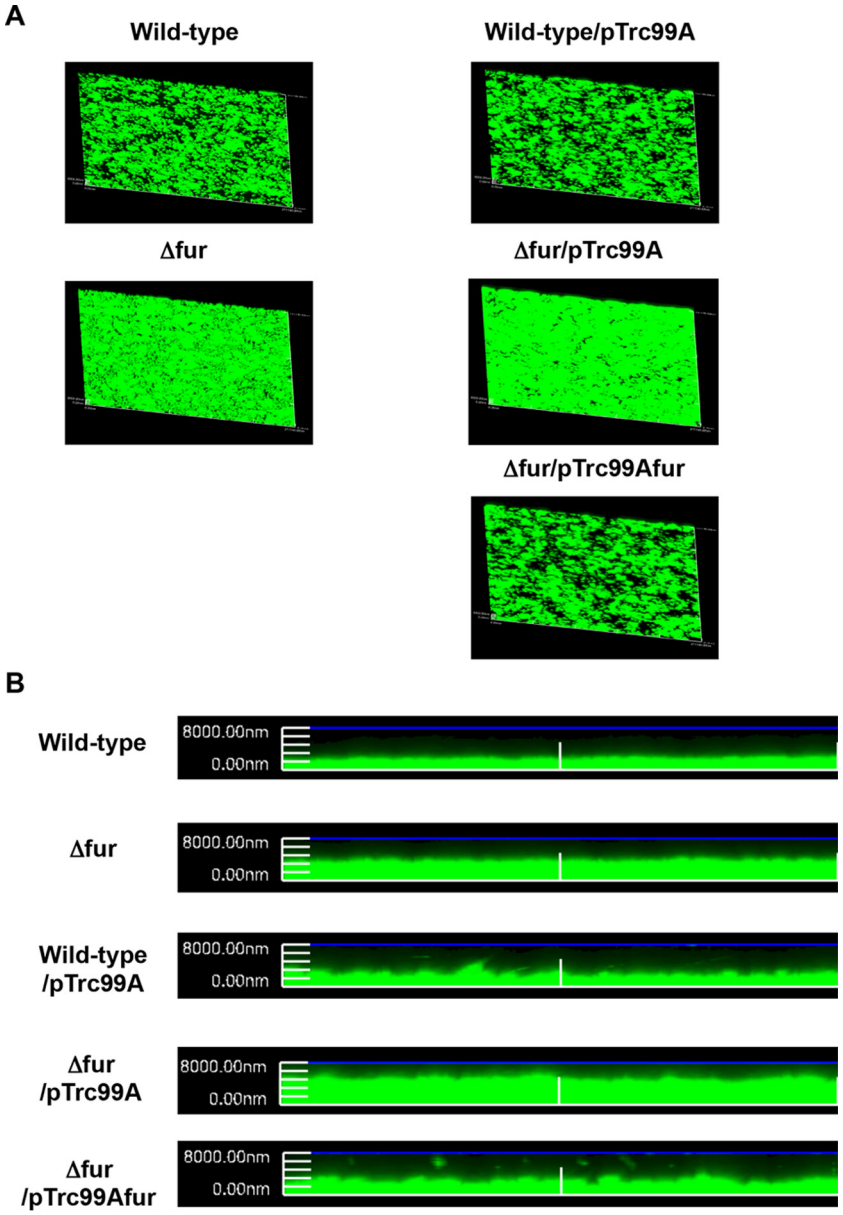

FIG 2 Attachment of the wild-type parent and the Δ*fur* mutant or the wild-type parent and the Δ*fur* mutant carrying pTrc99A (vector control) or pTrc99Afur (Fur expression plasmid) on coverslips. Bacteria stained with Syto9 were imaged as a green fluorescent color on the microscopy using a 60× objective. Overlooking (A) and cross-sectional (B) images were acquired for each sample. The experiment was repeated twice, and similar results were obtained.

parent after 24 h (Fig. 1B). Although no significant difference of CFU between the mutant and the wild-type parent for up to 8 h of culture was seen, the CFU count for the mutant was approximately 4-fold less than for the wild-type parent when their cultures were continued up to 24 h (data not shown). Therefore, the lower rate of attachment by the mutant cells after 24 h when grown in RPMI 1640 medium may have been due to a growth defect.

To confirm the contribution of the *fur* gene to bacterial adhesion, we introduced pTrc99Afur, a heterologous *fur* expression plasmid, into the Δ*fur* strain and performed static biofilm assays after 4 h of culture in RPMI 1640 medium. The rate of cell attachment by the Δ*fur* strain decreased to that of the wild-type strain carrying the empty vector when pTrc99Afur was introduced (Fig. 1C).

In addition to the static assays, living cells attached to glass coverslips were imaged by Syto9 staining using fluorescence confocal microscopy as described in Materials and Methods. After culture for 4 h, the Δ*fur* cells were attached more densely and thickly than the wild-type parent (Fig. 2A and B). When the pTrc99Afur plasmid was introduced, the degree of attachment of the Δ*fur* cells decreased to that of the wild-type parent carrying the empty vector. These observations suggest that the *fur* gene is a negative regulator of the initial attachment to the host cells and/or IBC development.

The *fur* mutant is highly adhesive and invasive. The increased attachment to polystyrene and glass surfaces by the deletion of *fur* might be associated with promotion of adhesion and invasion to the host cells. To test this hypothesis, we determined CFU for the

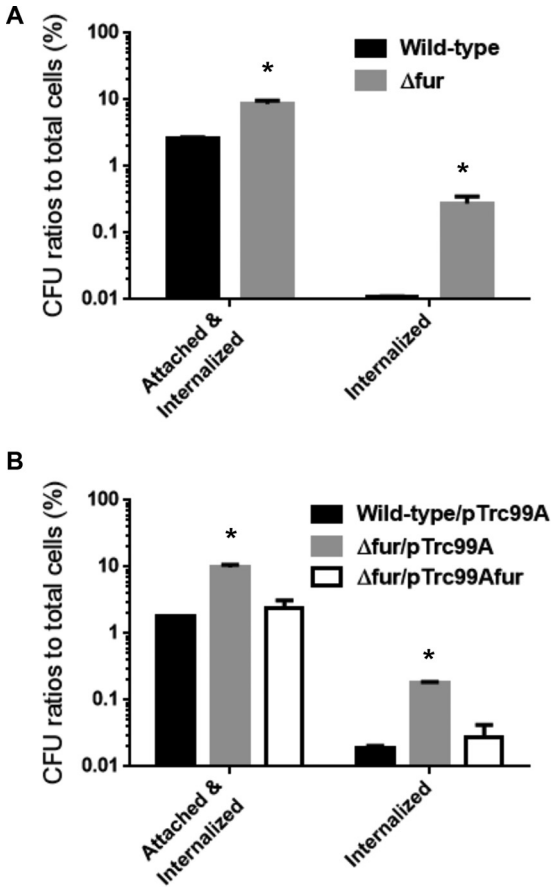

FIG 3 Adhesion to and invasion of bladder epithelial cells for the wild-type parent and the *fur* mutant (A) or the wild-type parent and the *fur* mutant carrying pTrc99A (vector control) or pTrc99Afur (Fur expression plasmid) (B). The *y* axis on each graph shows percent CFU of attached and internalized bacteria relative to total bacterial cell numbers. Data are the means from three independent experiments; error bars indicate the standard deviations. *, $P <$ 0.01 relative to the value for the wild-type control.

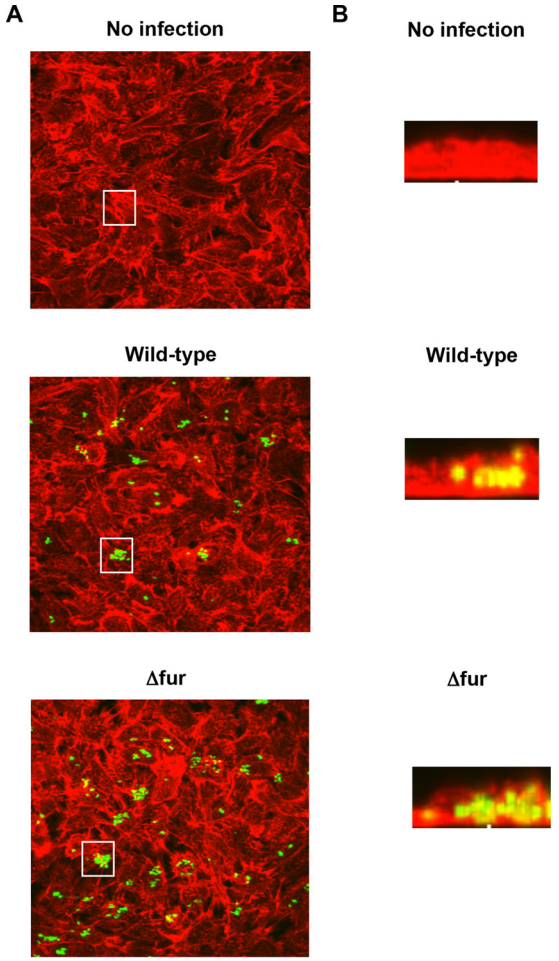

FIG 4 Fluorescent images of intracellular bacterial community (IBC) in the bladder epithelial cells (HTB-9). Bacteria carrying a green fluorescent protein (GFP) expression plasmid, pTurboGFP-B, and HTB-9 stained with rhodamine phalloidin were imaged as, respectively, green and red fluorescent colors by microscopy using a 60× objective. Overlooking images (A) and cross-sectional images in the white box indicated in panel A (B) were acquired for each sample. The experiment was repeated twice, and similar results were obtained.

wild-type parent and *fur* mutant when inoculated onto bladder epithelial cells using the gentamicin protection assays as described in Materials and Methods. The infection rates were compared based on the percentage of adhering and invading bacteria in epithelial cells relative to the total bacterial cells. The *fur* mutant showed a 3.3-fold-higher adhesive/invasive rate (2.6% ± 0.1% for the wild-type parent versus 8.6% ± 0.7% for the *fur* mutant) and a 28-fold-higher invasive rate (0.01% ± 0.002% for the wild-type parent versus 0.28% ± 0.05% for the *fur* mutant) than the wild-type parent (Fig. 3A). When the pTrc99Afur plasmid was introduced into the mutant, rates of adhesion and invasion were similar to those of the wild-type parent (adhesive/invasive rate, 1.8% ± 0.02% for the wild-type parent carrying the pTrc99A empty vector versus 9.8% ± 0.7% for the *fur* mutant carrying pTrc99A and 2.4% ± 0.5% for the *fur* mutant carrying pTrc99Afur; invasive rate, 0.02% ± 0.002% for the wild-type parent carrying the pTrc99A empty vector versus 0.18% ± 0.01% for the *fur* mutant carrying pTrc99A and 0.03% ± 0.01% for the *fur* mutant carrying pTrc99Afur) (Fig. 3B).

To evaluate IBC formation by the wild-type parent and *fur* mutant in bladder epithelial cells, we infected host cells with the GFP-expressing wild-type parent or Δ*fur* strain and then imaged the bacterial colonies and actin in the host epithelial cells. Consistent with the results from the gentamicin protection assays, the Δ*fur* construct was observed more frequently in host cells than the wild-type parent, and the IBC colonies formed by the mutant were relatively larger and denser than those formed by the wild-type parent (Fig. 4).

These observations suggest that the *fur* gene confers a negative effect on adhesion, invasion, and IBC formation in bladder epithelial cells.

The *fur* mutant has a higher level of expression of type 1 fimbriae. Type 1 and P-type fimbriae are major elements required for UPEC adhesion, invasion, and IBC formation (22). We therefore examined the effect of *fur* deletion on fimbria expression. Quantitative PCR (qPCR) analyses showed that the transcript levels of *fimA* and *fimH*, which encode the type 1 fimbrial major subunit and adhesin, respectively, were 2.0- and 2.2-fold higher in the *fur* mutant than those in the wild-type parent, while no significant

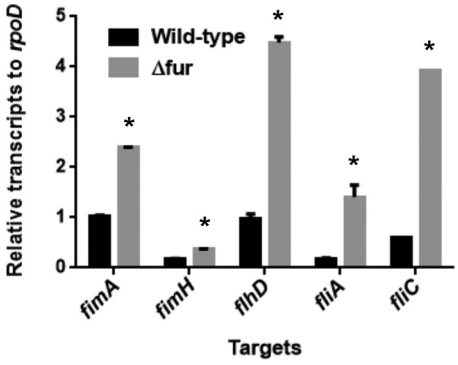

FIG 5 Transcript levels of fimbrial and motility-related genes in the wild-type parent and the *fur* mutant. Transcript levels are relative to that of *rpoD* (housekeeping gene). Data are the means of two biological replicates; error bars indicate the ranges. *, $P < 0.01$ relative to the value for the wild-type control.

increase in the transcript levels of *papA* and *papG*, which encode P-type fimbrial components, between the strains was observed (Fig. 5 and data not shown). *fimA* and *fimH* are cotranscribed from an operon, and the orientation of their promoter located at the region upstream of *fimA* is invertible ("ON" means that the promoter activity is ON and "OFF" means that the promoter activity is OFF) (21). We compared the populations of the wild-type parent and *fur* mutant with the promoter in the ON orientation. PCR-based phase variation assays as described in Materials and Methods are able to distinguish the ON orientation as 489-bp and 70-bp DNA fragments and the OFF orientation as 359-bp and 200-bp DNA fragments (Fig. 6). We found that the population of cells with the ON orientation for the mutant was higher than that for the wild-type parent (Fig. 6). When the *fur* gene was expressed from the pTrc99Afur plasmid in the mutant strain, the population of cells with the ON orientation decreased to the level of the wild-type parent carrying the empty vector. Type 1 fimbriae can hemagglutinate guinea pig RBCs; however, the hemagglutination is inhibited in the presence of mannose because mannose blocks the interaction between FimH and the mannosylated receptor on the RBCs (23). We used hemagglutination assays to estimate the activity of the type 1 fimbriae produced by the wild-type parent and *fur* mutant in the presence or absence of mannose. The mutant cells hemagglutinated the guinea pig RBCs at an 8-fold-higher titer than the wild-type parent when they were resuspended in mannose-free PBS (titers: 32 for the wild-type parent and 256 for the *fur* mutant); however, the titer decreased in the presence of mannose, and then no difference between the wild-type parent and the mutant was seen (titers: 1 for the wild-type parent and 1 for the *fur* mutant) (Table 3). We confirmed that the titer elevated by the *fur* gene deletion was decreased to the level of the wild-type parent by heterologous expression of the *fur* gene on the pTrc99Afur plasmid. These combined results indicate that type 1 fimbriae are produced at higher numbers in the *fur* mutant and lead to promoted adhesion, invasion, and IBC formation in the host cells.

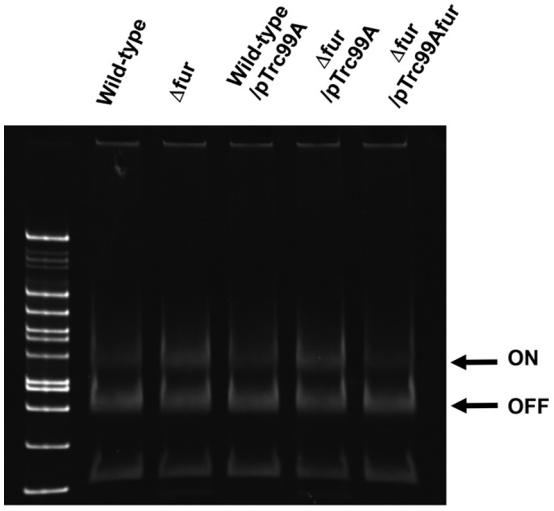

FIG 6 Phase variation of type I fimbrial gene promoter in the wild-type parent and the *fur* mutant or the wild-type parent and the *fur* mutant carrying pTrc99A (vector control) or pTrc99Afur (Fur expression plasmid) when cultured in RPMI 1640 medium. PCR-amplified samples prepared as described in Materials and Methods were digested by HinfI and separated on polyacrylamide gels. The DNAs were visualized by SYBR green I staining under UV light at 300 nm.

TABLE 3 HA titers of the wild-type parent and the *fur* mutant

Strain	HA titer	
	Without mannose	With mannose
Wild type	32	1
Δ*fur* mutant	256	1
Wild type carrying pTrc99A	32	1
Δ*fur* mutant carrying pTrc99A	256	1
Δ*fur* mutant carrying pTrc99Afur	32	1

Deletion of the *fur* gene increases motilities. Flagella provide a positive effect on biofilm formation in *E. coli* because nonflagellated mutants that lack motility produce a smaller biomass on the surface (24). Flagella help bacteria disperse from the biofilm matrix and settle in more suitable niches. Thus, we hypothesize that motility and flagellar expression might be increased in the *fur* mutant. To test this hypothesis, we compared the motilities on soft agar plates for these strains. The results showed that the mutant had greater motility than the wild-type parent (diameters: 42 ± 1 mm for the wild-type parent and 61 ± 2 mm for the *fur* mutant) (Fig. 7). When a plasmid containing the *fur* gene was introduced into the mutant, the motility decreased to that of the wild-type parent (diameters: 34 ± 4 mm for the wild type parent carrying pTrc99A, 61 ± 2 mm for the *fur* mutant carrying pTrc99A, and 21 ± 1 mm for the *fur* mutant carrying pTrc99Afur) (Fig. 7). In agreement with motility assays, quantitative PCR analyses detected higher levels of expression of *flhD* and *fliA* (which encode regulatory elements for flagellar expression) and *fliC* (which encodes a major flagellar component) (25) in the *fur* mutant than in the wild-type parent (Fig. 5).

Fur binds to the region upstream of the *fimA* gene. To determine if Fur directly represses the expression of *fimA* and *fimH*, *flhD*, *fliA*, and *fliC*, we tested the ability of Fur to bind to the regions upstream of these genes using a gel shift assay. We observed a retarded mobility of the *fimA* and *fimH* and *flhD* upstream regions, but not of *fliA* and *fliC*, or *torC* as a nonspecific control (Fig. 8A). Fur is proposed to bind to the consensus sequence (5′-GATAATGATAATCATTATC-3′) (26). We found a

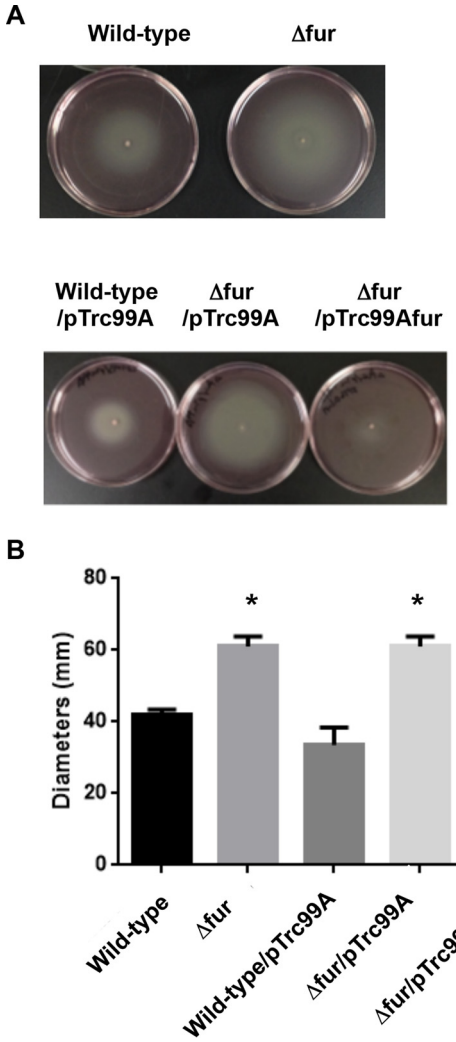

FIG 7 Motilities of the wild-type parent and *fur* mutant and these strains carrying pTrc99A (vector control) or pTrc99Afur (Fur expression plasmid). (A) Bacterial migrations on RPMI 1640 medium containing 0.3% agar after 8 h at 37°C under 5% CO_2. (B) Bacterial migrations on the agar, represented as diameters. Data are the means from three independent experiments; error bars indicate the standard deviations. *, $P < 0.01$ relative to the value for the wild-type control.

similar sequence (GATAACTATAGAACATTAAG) at 244 bp upstream of the *fimA* transcriptional start site (Fig. 8B). This site partially overlapped with a sequence recognized by Lrp that induces phase variation in the *fimA* promoter (27). Thus, Fur binding to the *fimA* promoter region may interfere with Lrp-induced phase variation, thereby reducing *fimA* transcription. To test this hypothesis, we constructed an *lrp* mutant and compared the transcript levels of *fimA* and *fimH* in the wild-type parent and Δ*lrp*, Δ*fur*, and Δ*fur* Δ*lrp* strains by qPCR analyses. As expected, the deletion of *lrp* from both the wild-type and Δ*fur* backgrounds decreased the levels of *fimA* and *fimH* expression; however, the transcript levels of these two genes were still higher in the Δ*fur* Δ*lrp* strain than in the Δ*lrp* strain (Fig. 8C). Therefore, Fur most likely does not affect the action of Lrp, such as interference of phase variation via binding competition. On the other hand, there was no similar conserved consensus sequence that Fur probably binds on the region upstream of *flhD*. Therefore, we suggest that Fur has very low affinity for the *flhD* promoter because approximately 50% of the DNA band pool from *fimA* promoter was shifted even in the presence of 10 pmol of Fur, while a significant amount of the unshifted *flhD* fragment was still observed at the same concentration (Fig. 8A). The repression of *flhD* promoter by Fur might be dominantly indirect in physiological situations.

Adhesion, invasion, and motility of UPEC are promoted under iron-depleted conditions via inactivation of Fur. Fur forms a complex with ferrous iron and then represses the gene expression of specific targets (13). However, when available iron is limited, Fur is dissociated and the expression of the target genes is derepressed. Thus, we tested whether adhesion, invasion, and motility of UPEC are promoted when iron is depleted as the *fur* mutant showed. To deplete iron from the bacterial culture, we added 2,2-dipyridyl, an iron chelator, to the media used for precultures and assays. When 2,2-dipyridyl was added to the wild-type UPEC cultures, the rates of attachment to the 96-well plate, adhesion to and invasion of the bladder epithelial cells, and motility on agar plates were elevated up to the level of the *fur* mutant (Fig. 9). On the other hand, further elevation of those rates was not observed in the *fur* mutant background in spite of 2,2-dipyridyl addition. These results indicate that inactivation of Fur followed by iron depletion derepresses adhesion, invasion, and IBC formation in bladder epithelial cells and motility.

Elevation of attachment and invasion by the *fur* gene deletion is not due to overexpression of RyhB. Fur is a repressor of RyhB, a noncoding small regulatory RNA. The RNA controls a subset of genes encoding proteins that require iron as a cofactor for their activities (28). We tested if overexpression of RyhB promotes attachment and invasion because deletion of *fur* leads to elevation of RyhB transcription (29). We constructed two plasmids for RyhB overexpression as described in Materials and Methods. For the first plasmid, the *ryhB* gene was cloned downstream of the *trc* promoter in the pTrc99A vector to generate pTrc99AryhB; this made it possible for *ryhB* transcription to be activated by IPTG. For the second plasmid, we inserted the *ryhB* gene into a multicloning site in the pUC19 vector, a very-high-copy-number plasmid, to generate pUC19ryhB. Static biofilm assays showed that there was no difference in the rate of attachment to 96-well polystyrene plates for the wild-type parent carrying each RyhB overexpression plasmid and the vector control (see Fig. S1A in the supplemental material). There was no significant difference in the growth rates of these strains (see Fig. S1B). In experiments using the *ryhB* mutant described below, the Δ*fur* Δ*ryhB* double mutant still exhibited increased attachment and invasion rates in the same manner as the Δ*fur* single mutant (see Fig. S1A and C). These observations suggest that the enhanced attachment and invasion observed in the *fur* mutant were not due to overexpression of RyhB.

In addition to RyhB overexpression, we used static biofilm assays to measure the rate of attachment in the *ryhB* deletion mutant when cultured in RPMI 1640 medium for 4 h as in the experiment whose results are shown in Fig. 1C. Interestingly, the mutant exhibited a higher rate of attachment than the wild-type parent (see Fig. S1A). The growth rate of the *ryhB* mutant was the same as that of the wild-type parent (see Fig. S1B). We also compared adherence to and invasion of the bladder epithelial cells between the wild-type parent and the mutant by gentamicin protection assays.

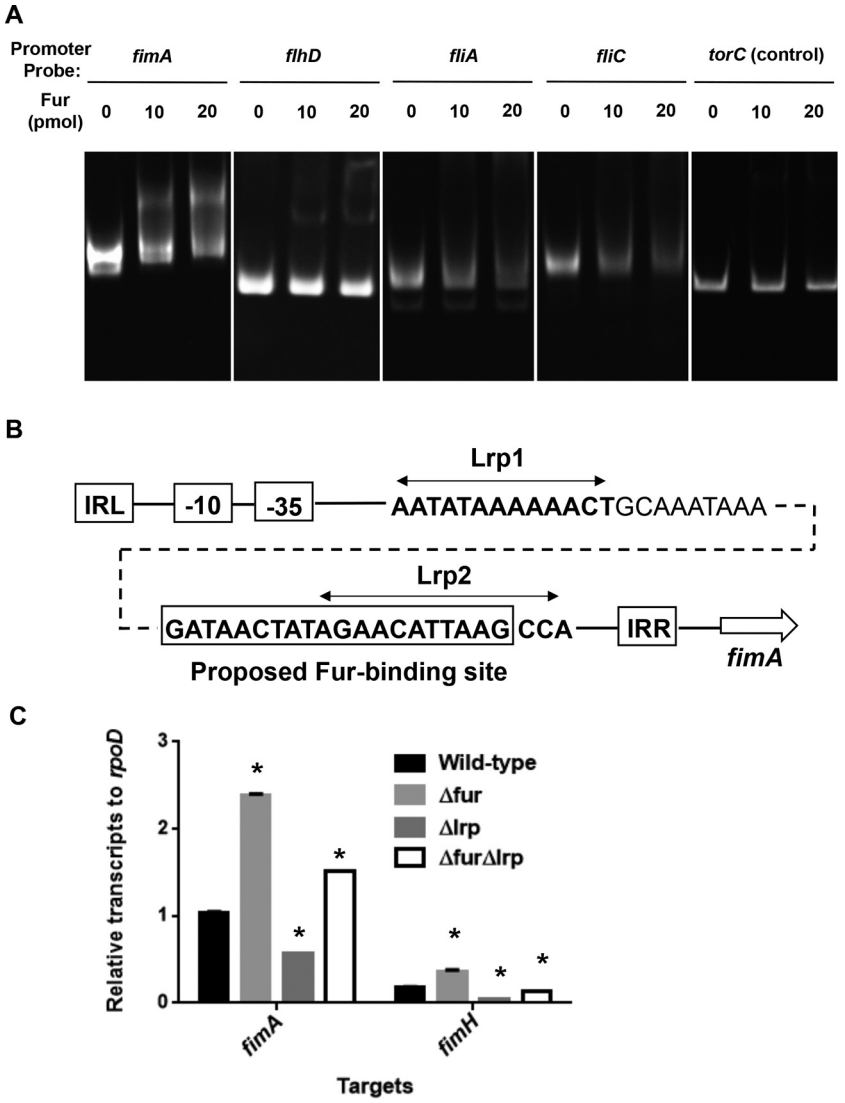

FIG 8 Fur binds to the *fimA* upstream region containing Lrp-binding sequence. (A) Gel shift assay showing binding of Fur to the region upstream of *fimA*, *flhD*, *fliA*, and *fliC*. The Fur protein (0, 10, or 20 pmol) was added to reaction mixtures containing 0.3 pmol of DNA probe. DNA upstream of *torC* was used as a nonbinding (negative) control. Reaction mixtures were separated on polyacrylamide gels. Free and Fur-bound DNAs were visualized by SYBR green I staining under UV of 300 nm. (B) Localization of Fur and Lrp-binding sites in the *fimA* upstream region. The converging bold arrows indicate the Lrp binding sites, and the predicted Fur-binding site is indicated by the box in the "OFF" orientation of *fim*-phase variation. The predicted −10 and −35 boxes on *fimA* promoter are indicated. IRR, inverted repeat right; IRL, inverted repeat left. (C) Transcript levels of *fimA* and *fimH* in the wild-type parent and Δ*fur*, Δ*lrp*, and Δ*fur* Δ*lrp* mutants. Transcript levels are relative to that of *rpoD* (housekeeping gene). Data are the means of two biological replicates; error bars indicate the ranges. *, $P < 0.01$ relative to the value for the wild-type control.

Consistent with the results from the static biofilm assays, the *ryhB* mutant adhered to and invaded the bladder epithelial cells in higher numbers than the wild-type parent strain (see Fig. S1C). In addition, we found that the *ryhB* mutant had higher transcription levels of *flhD*, *fliA*, and *fliC* than the wild-type parent as determined by qPCR and actually exhibited higher motility (see Fig. S1D and E). However, there were no significant differences in transcript levels of *fimA* and *fimH* in the wild-type parent and the *ryhB* mutant (see Fig. S1D). These observations suggest that the increased attachment and invasion by *ryhB* gene deletion were not due to elevated expression of type I fimbriae, unlike in the case of *fur* gene deletion.

DISCUSSION

The intracellular iron concentration is strictly controlled in bacteria because diverse essential and nonessential metabolic enzymes require iron as a cofactor for their enzymatic activities, while excess iron generates hydroxyl radical species via the Fenton reaction and causes oxidative damage in cells (12). Fur represses genes encoding proteins contributing to iron uptake and iron-dependent metabolic enzymes when iron is abundantly available, and it is highly conserved in many bacterial species (13). Associated with its native function, Fur is involved in pathogenesis for some pathogens, such as *Staphylococcus aureus* (14). In those cases, it provides a benefit for virulence because deletion of the *fur*

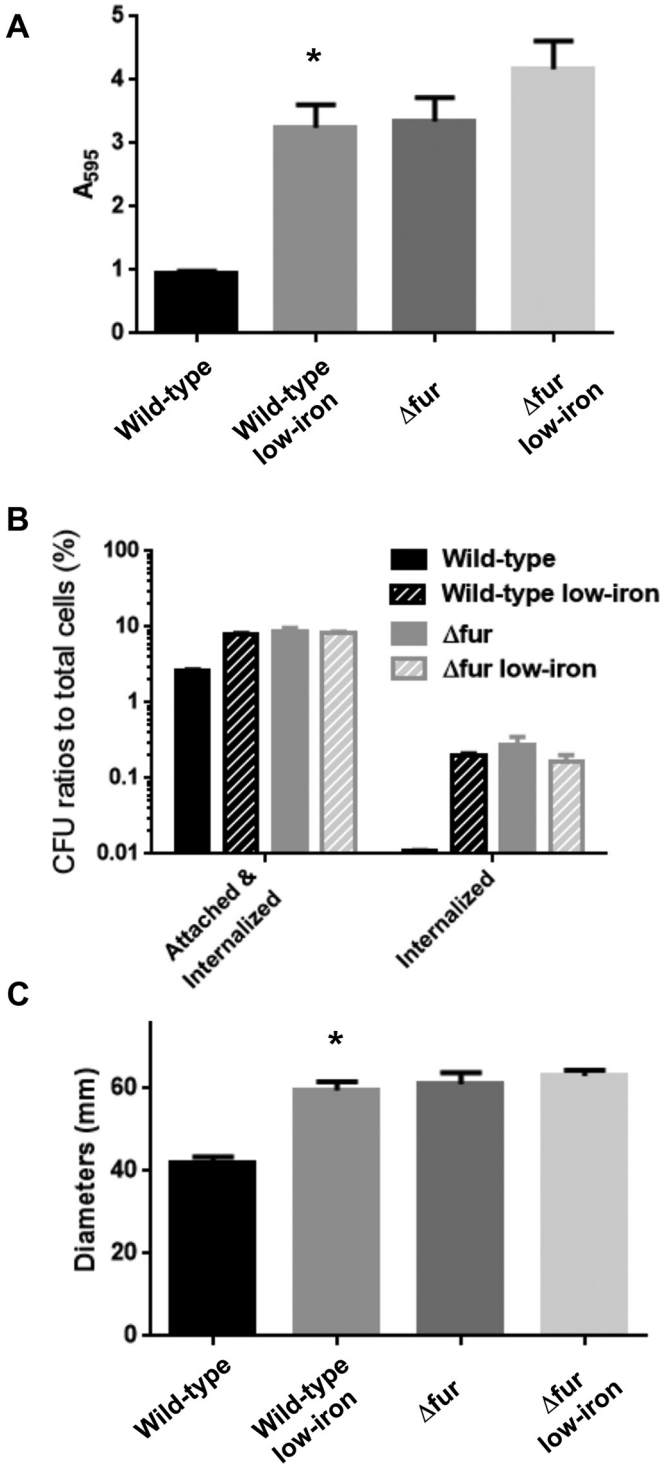

FIG 9 Attachment, invasion, and motilities of the wild-type parent and *fur* mutant under normal or iron-depleted conditions. (A) Rates of attached bacteria on 96-well polystyrene plate when cultured in the presence or absence of 0.1 mM 2,2-dipyridyl, an iron chelator, in RPMI 1640 medium. These rates are represented as A_{595} values normalized to an OD_{600} of 1. Data are the means of three biological replicates; error bars indicate the ranges. *, $P < 0.01$ for values for bacterial cultures under iron-depleted conditions relative to those under normal conditions. (B) Rates of adhering and invading bacteria in the bladder epithelial cells in the presence or absence of 0.2 mM 2,2-dipyridyl. The *y* axis on each graph shows percent CFU for adhered and internalized bacteria relative to total bacterial cell numbers. Data are the means from three independent experiments; error bars indicate the standard deviations. *, $P < 0.01$ for values for bacterial cultures under iron-depleted conditions relative to those under normal conditions. (C) Motilities of the wild-type parent and *fur* mutant cultured in the presence or absence of 0.1 mM 2,2-dipyridyl. Bacterial migrations on the agar are represented as diameters. Data are the means from three independent experiments; error bars indicate the standard deviations. *, $P < 0.01$ for values for bacterial cultures under iron-depleted conditions relative to those under normal conditions.

gene attenuates virulence. Therefore, Fur is expected to be a potential target for antibacterial chemotherapy. The virulence might be attenuated if we block the activity of Fur in any way.

However, there may be challenges to demonstrating the potential efficacy of Fur inhibitors for UTIs caused by UPEC. An *in vivo* study of UPEC using a mouse model showed that the deletion of *fur* did not attenuate UPEC virulence during UTIs because the *fur* mutant formed a number of colonies in the bladder similar to that of the wild-type strain (30). Both *in vivo* and *in vitro* studies using clinical and laboratory UPEC strains showed that siderophore production is necessary for virulence (31, 32). Efficient iron acquisition via siderophores allows bacteria to survive and grow. Bacterial siderophores compete with lipocalin 2 (Lcn2), which is secreted by host cells as an innate defense system that sequesters iron from enterobactin complexes (33, 34). Siderophore production is suppressed by Fur under iron-rich conditions and induced when iron is restricted. This implies that the Fur activity in UPEC cells could be low during UTIs because most portions of the Fur protein pool are dissociated from iron due to its limited availability in the urinary tract (35).

On the other hand, the results from our *in vitro* approach suggest that *fur* deletion increases adhesion to and invasion of the bladder epithelial cells and enhances motility in an iron-rich medium (Fig. 1 to 4 and 7). When iron was depleted from the medium, the attachment, invasion, and motility of the wild-type parent were enhanced, whereas those of the *fur* mutant were not further enhanced (Fig. 9). Fur is a negative regulator of virulence in UPEC when sufficient iron is available in the environment, but the virulence of the bacterium is derepressed in iron-restricted situations such as in patients with UTIs. Thus, the pathogenicity of UPEC in UTIs might already include enhanced virulence due to Fur inactivation. Consequently, we suggest that inhibition of Fur activity may not be an efficient antibacterial approach to treating UTIs caused by UPEC. However, disruption of Fur activity imposes fitness costs on cells due to the constitutive expression of the iron uptake system. Therefore, a Fur inhibitor might be still potentially useful for treating infections in sites where iron is relatively abundant, for instance, as in bacteremia.

How does deletion of *fur* derepress attachment, invasion, IBC formation, and motility? We provided evidence that a recombinant Fur protein bound to the region upstream of *fimA* and led to reduction of type 1 fimbrial expression, likely via the direct inhibition of *fimA* transcriptional initiation and negative control of phase variation but without affecting the action of Lrp, while transcription of *flhD*, which encodes a positive regulator of flagellar gene expression that contributes to motility, was also directly repressed (Fig. 5 and 6). Thus, the enhanced attachment, invasion, IBC formation, and motility of UPEC produced by deleting the *fur* gene can be explained by derepression of fimbrial and flagellar genes. Other studies have shown that the salmochelin siderophore

receptor, IroN, and the homolog protein of IrgA adhesin, Iha, whose expression is repressed by Fur, promote the invasion of uroepithelial cells and biofilm formation and adherence to uroepithelial cells, respectively (36–39). Therefore, IroN and Iha might also participate in the hypervirulent phenotypes of the *fur* mutant analyzed in our study.

Inactivation of Fur leads to the overexpression of RyhB under iron-depleted conditions (28). However, our results from experiments using RyhB overexpression strains and a Δ*fur* Δ*ryhB* mutant suggested that the enhanced attachment, invasion, and motility observed in the *fur* mutant are not due to the overexpression of RyhB (see Fig. S1A to C in the supplemental material). Interestingly, deletion of the *ryhB* gene rather enhanced attachment to and invasion of the bladder epithelial cells and motility (see Fig. S1A to C and E). Unlike the case with the *fur* mutant, the deletion of *ryhB* increased the expression of flagellar genes but not fimbrial genes. In contrast, the *ryhB* mutant formed a lower number of colonies than the wild type in the bladders of mice (30). RyhB represses the expression of nonessential iron-using metabolic enzymes under low-iron conditions and then increases the availability of iron for essential iron-using metabolic enzymes (28). Therefore, we speculate that deletion of *ryhB* might increase the iron-associated metabolic cost that causes fitness disadvantages in the mouse bladder, where iron is relatively limited, and then counteract the benefits of enhanced virulence phenotypes, including attachment, invasion, and motility. Although we still do not know how RyhB controls virulence-associated flagellar gene expression without affecting fimbrial expression, this will be the basis of future studies.

In this study, we elucidated the role of Fur in UPEC virulence based on *in vitro* analyses. We believe that insights into the molecular mechanism of Fur-mediated virulence control based on both *in vivo* and *in vitro* approaches will aid us in precisely evaluating its potency as a drug target for treating bacterial infections.

ACKNOWLEDGMENTS

This study was kindly supported by a JSPS KAKENHI Grant-in-Aid for Young Scientists (B) (grant 25870115, JST program), the program Improvement of Research Environment for Young Researchers, the Japanese Ministry of Education, Culture, Sports, Science and Technology (Gunma University operation grants), a GlaxoSmithKline (GSK) research grant, the Takeda Science Foundation, and the Research Program on Emerging and Re-Emerging Infectious Diseases from the Japan Agency of Research and Development (AMED).

FUNDING INFORMATION

This work, including the efforts of Hidetada Hirakawa, was funded by JSPS KAKENHI (25870115).

REFERENCES

1. **Hayami H, Takahashi S, Ishikawa K, Yasuda M, Yamamoto S, Uehara S, Hamasuna R, Matsumoto T, Minamitani S, Watanabe A, Iwamoto A, Totsuka K, Kadota J, Sunakawa K, Sato J, Hanaki H, Tsukamoto T, Kiyota H, Egawa S, Tanaka K, Arakawa S, Fujisawa M, Kumon H, Kobayashi K, Matsubara A, Naito S, Tatsugami K, Yamaguchi T, Ito S, Kanokogi M, Narita H, Kawano H, Hosobe T, Takayama K, Sumii T, Fujii A, Sato T, Yamauchi T, Izumitani M, Chokyu H, Ihara H, Akiyama K, Yoshioka M, Uno S, Monden K, Kano M, Kaji S, Kawai S, Ito K, Inatomi H, Nishimura H, Ikuyama T, Nishi S, Takahashi K, Kawano Y, Ishihara S, Tsuneyoshi K, Matsushita S, Yamane T, Hirose T, Fujihiro S, Endo K, Oka Y, Takeyama K, Kimura T, Uemura T.** 2013. Nationwide surveillance of bacterial pathogens from patients with acute uncomplicated cystitis conducted by the Japanese surveillance committee during 2009 and 2010: antimicrobial susceptibility of *Escherichia coli* and *Staphylococcus saprophyticus*. J Infect Chemother **19:**393–403. http://dx.doi.org/10.1007/s10156-013-0606-9.
2. **Zhang L, Foxman B.** 2003. Molecular epidemiology of *Escherichia coli* mediated urinary tract infections. Front Biosci **8:**e235–e44. http://dx.doi.org/10.2741/1007.
3. **Justice SS, Hung C, Theriot JA, Fletcher DA, Anderson GG, Footer MJ, Hultgren SJ.** 2004. Differentiation and developmental pathways of uropathogenic *Escherichia coli* in urinary tract pathogenesis. Proc Natl Acad Sci U S A **101:**1333–1338. http://dx.doi.org/10.1073/pnas.0308125100.
4. **Anderson GG, Palermo JJ, Schilling JD, Roth R, Heuser J, Hultgren SJ.** 2003. Intracellular bacterial biofilm-like pods in urinary tract infections. Science **301:**105–107. http://dx.doi.org/10.1126/science.1084550.
5. **Mulvey MA, Lopez-Boado YS, Wilson CL, Roth R, Parks WC, Heuser J, Hultgren SJ.** 1998. Induction and evasion of host defenses by type 1-piliated uropathogenic *Escherichia coli*. Science **282:**1494–1497. http://dx.doi.org/10.1126/science.282.5393.1494.
6. **Mulvey MA, Schilling JD, Hultgren SJ.** 2001. Establishment of a persistent *Escherichia coli* reservoir during the acute phase of a bladder infection. Infect Immun **69:**4572–4579. http://dx.doi.org/10.1128/IAI.69.7.4572-4579.2001.
7. **Martinez JJ, Mulvey MA, Schilling JD, Pinkner JS, Hultgren SJ.** 2000. Type 1 pilus-mediated bacterial invasion of bladder epithelial cells. EMBO J **19:**2803–2812. http://dx.doi.org/10.1093/emboj/19.12.2803.
8. **Wright KJ, Seed PC, Hultgren SJ.** 2007. Development of intracellular bacterial communities of uropathogenic *Escherichia coli* depends on type 1 pili. Cell Microbiol **9:**2230–2241. http://dx.doi.org/10.1111/j.1462-5822.2007.00952.x.
9. **Lane MC, Lockatell V, Monterosso G, Lamphier D, Weinert J, Hebel JR, Johnson DE, Mobley HL.** 2005. Role of motility in the colonization of uropathogenic *Escherichia coli* in the urinary tract. Infect Immun **73:**7644–7656. http://dx.doi.org/10.1128/IAI.73.11.7644-7656.2005.
10. **Wright KJ, Seed PC, Hultgren SJ.** 2005. Uropathogenic *Escherichia coli* flagella aid in efficient urinary tract colonization. Infect Immun **73:**7657–7668. http://dx.doi.org/10.1128/IAI.73.11.7657-7668.2005.
11. **Lane MC, Alteri CJ, Smith SN, Mobley HL.** 2007. Expression of flagella is coincident with uropathogenic *Escherichia coli* ascension to the upper urinary tract. Proc Natl Acad Sci U S A **104:**16669–16674. http://dx.doi.org/10.1073/pnas.0607898104.
12. **Andrews SC, Robinson AK, Rodriguez-Quinones F.** 2003. Bacterial iron homeostasis. FEMS Microbiol Rev **27:**215–237. http://dx.doi.org/10.1016/S0168-6445(03)00055-X.
13. **Bagg A, Neilands JB.** 1987. Ferric uptake regulation protein acts as a repressor, employing iron (II) as a cofactor to bind the operator of an iron transport operon in *Escherichia coli*. Biochemistry **26:**5471–5477. http://dx.doi.org/10.1021/bi00391a039.
14. **Porcheron G, Dozois CM.** 2015. Interplay between iron homeostasis and virulence: Fur and RyhB as major regulators of bacterial pathogenicity. Vet Microbiol **179:**2–14. http://dx.doi.org/10.1016/j.vetmic.2015.03.024.
15. **Welch RA, Burland V, Plunkett G, III, Redford P, Roesch P, Rasko D, Buckles EL, Liou SR, Boutin A, Hackett J, Stroud D, Mayhew GF, Rose DJ, Zhou S, Schwartz DC, Perna NT, Mobley HL, Donnenberg MS, Blattner FR.** 2002. Extensive mosaic structure revealed by the complete genome sequence of uropathogenic *Escherichia coli*. Proc Natl Acad Sci U S A **99:**17020–17024. http://dx.doi.org/10.1073/pnas.252529799.
16. **Fogh J.** 1978. Cultivation, characterization, and identification of human tumor cells with emphasis on kidney, testis, and bladder tumors. Natl Cancer Inst Monogr **49:**5–9.
17. **Link AJ, Phillips D, Church GM.** 1997. Methods for generating precise deletions and insertions in the genome of wild-type *Escherichia coli*: application to open reading frame characterization. J Bacteriol **179:**6228–6237.
18. **Hirakawa H, Nishino K, Hirata T, Yamaguchi A.** 2003. Comprehensive studies of drug resistance mediated by overexpression of response regulators of two-component signal transduction systems in *Escherichia coli*. J Bacteriol **185:**1851–1856. http://dx.doi.org/10.1128/JB.185.6.1851-1856.2003.
19. **Yanisch-Perron C, Vieira J, Messing J.** 1985. Improved M13 phage cloning vectors and host strains: nucleotide sequences of the M13mp18 and pUC19 vectors. Gene **33:**103–119. http://dx.doi.org/10.1016/0378-1119(85)90120-9.
20. **O'Toole GA.** 2011. Microtiter dish biofilm formation assay. J Vis Exp **30:**2437.
21. **Struve C, Krogfelt KA.** 1999. In vivo detection of *Escherichia coli* type 1

fimbrial expression and phase variation during experimental urinary tract infection. Microbiology **145**(Part 10):2683–2690.
22. **Lillington J, Geibel S, Waksman G.** 2014. Biogenesis and adhesion of type 1 and P pili. Biochim Biophys Acta **1840:**2783–2793. http://dx.doi.org/10.1016/j.bbagen.2014.04.021.
23. **Hultgren SJ, Schwan WR, Schaeffer AJ, Duncan JL.** 1986. Regulation of production of type 1 pili among urinary tract isolates of *Escherichia coli*. Infect Immun **54:**613–620.
24. **Pratt LA, Kolter R.** 1998. Genetic analysis of *Escherichia coli* biofilm formation: roles of flagella, motility, chemotaxis and type I pili. Mol Microbiol **30:**285–293. http://dx.doi.org/10.1046/j.1365-2958.1998.01061.x.
25. **Macnab RM.** 1992. Genetics and biogenesis of bacterial flagella. Annu Rev Genet **26:**131–158. http://dx.doi.org/10.1146/annurev.ge.26.120192.001023.
26. **Lavrrar JL, Christoffersen CA, McIntosh MA.** 2002. Fur-DNA interactions at the bidirectional *fepDGC-entS* promoter region in *Escherichia coli*. J Mol Biol **322:**983–995. http://dx.doi.org/10.1016/S0022-2836(02)00849-5.
27. **Blomfield IC, Kulasekara DH, Eisenstein BI.** 1997. Integration host factor stimulates both FimB- and FimE-mediated site-specific DNA inversion that controls phase variation of type 1 fimbriae expression in *Escherichia coli*. Mol Microbiol **23:**705–717. http://dx.doi.org/10.1046/j.1365-2958.1997.2241615.x.
28. **Massé E, Escorcia FE, Gottesman S.** 2003. Coupled degradation of a small regulatory RNA and its mRNA targets in *Escherichia coli*. Genes Dev **17:**2374–2383. http://dx.doi.org/10.1101/gad.1127103.
29. **Massé E, Gottesman S.** 2002. A small RNA regulates the expression of genes involved in iron metabolism in *Escherichia coli*. Proc Natl Acad Sci U S A **99:**4620–4625. http://dx.doi.org/10.1073/pnas.032066599.
30. **Porcheron G, Habib R, Houle S, Caza M, Lepine F, Daigle F, Masse E, Dozois CM.** 2014. The small RNA RyhB contributes to siderophore production and virulence of uropathogenic *Escherichia coli*. Infect Immun **82:**5056–5068. http://dx.doi.org/10.1128/IAI.02287-14.
31. **Garcia EC, Brumbaugh AR, Mobley HL.** 2011. Redundancy and specificity of *Escherichia coli* iron acquisition systems during urinary tract infection. Infect Immun **79:**1225–1235. http://dx.doi.org/10.1128/IAI.01222-10.
32. **Henderson JP, Crowley JR, Pinkner JS, Walker JN, Tsukayama P, Stamm WE, Hooton TM, Hultgren SJ.** 2009. Quantitative metabolomics reveals an epigenetic blueprint for iron acquisition in uropathogenic *Escherichia coli*. PLoS Pathog **5:**e1000305. http://dx.doi.org/10.1371/journal.ppat.1000305.
33. **Flo TH, Smith KD, Sato S, Rodriguez DJ, Holmes MA, Strong RK, Akira S, Aderem A.** 2004. Lipocalin 2 mediates an innate immune response to bacterial infection by sequestrating iron. Nature **432:**917–921. http://dx.doi.org/10.1038/nature03104.
34. **Fischbach MA, Lin H, Zhou L, Yu Y, Abergel RJ, Liu DR, Raymond KN, Wanner BL, Strong RK, Walsh CT, Aderem A, Smith KD.** 2006. The pathogen-associated *iroA* gene cluster mediates bacterial evasion of lipocalin 2. Proc Natl Acad Sci U S A **103:**16502–16507. http://dx.doi.org/10.1073/pnas.0604636103.
35. **Snyder JA, Haugen BJ, Buckles EL, Lockatell CV, Johnson DE, Donnenberg MS, Welch RA, Mobley HL.** 2004. Transcriptome of uropathogenic *Escherichia coli* during urinary tract infection. Infect Immun **72:**6373–6381. http://dx.doi.org/10.1128/IAI.72.11.6373-6381.2004.
36. **Feldmann F, Sorsa LJ, Hildinger K, Schubert S.** 2007. The salmochelin siderophore receptor IroN contributes to invasion of urothelial cells by extraintestinal pathogenic *Escherichia coli in vitro*. Infect Immun **75:**3183–3187. http://dx.doi.org/10.1128/IAI.00656-06.
37. **Magistro G, Hoffmann C, Schubert S.** 2015. The salmochelin receptor IroN itself, but not salmochelin-mediated iron uptake promotes biofilm formation in extraintestinal pathogenic *Escherichia coli* (ExPEC). Int J Med Microbiol **305:**435–445. http://dx.doi.org/10.1016/j.ijmm.2015.03.008.
38. **Johnson JR, Jelacic S, Schoening LM, Clabots C, Shaikh N, Mobley HL, Tarr PI.** 2005. The IrgA homologue adhesin Iha is an *Escherichia coli* virulence factor in murine urinary tract infection. Infect Immun **73:**965–971. http://dx.doi.org/10.1128/IAI.73.2.965-971.2005.
39. **Léveillé S, Caza M, Johnson JR, Clabots C, Sabri M, Dozois CM.** 2006. Iha from an *Escherichia coli* urinary tract infection outbreak clonal group A strain is expressed in vivo in the mouse urinary tract and functions as a catecholate siderophore receptor. Infect Immun **74:**3427–3436. http://dx.doi.org/10.1128/IAI.00107-06.